

Scaling of Transport Coefficients of Porous Media under Compaction

DENIS S. GOLDOBIN

Department of Mathematics, University of Leicester, Leicester LE1 7RH, UK
Institute of Continuous Media Mechanics, UB RAS, Perm 614013, Russia

PACS 47.56.+r – Fluid flow through porous media
PACS 92.40.Kf – Groundwater: aquifers
PACS 91.50.Hc – Marine geology: gas and hydrate systems

Abstract. – Porous sediments in geological systems are exposed to stress by the above-laying mass and consequent compaction, which may be significantly nonuniform across the massif. We derive scaling laws for the compaction of sediments of similar geological origin. With these laws, we evaluate the dependence of the transport properties of a fluid-saturated porous medium (permeability, effective molecular diffusivity, hydrodynamic dispersion, electrical and thermal conductivities) on its porosity. In particular, we demonstrate that the assumption of a uniform geothermal gradient is not adequate for systems with nonuniform compaction and show the importance of the derived scaling laws for mathematical modelling of methane hydrate deposits; these deposits are believed to have potential for impact on global climate change and Glacial-Interglacial cycles.

Introduction. – The reconstruction of properties of grounds is an important problem related to geological surveys for extraction of minerals and hydrocarbons, construction of buildings, forecasting geological hazards (seismic, erosion-related, anomalous impact on the climate, *etc.*) [1–3]. Dealing with this problem one faces challenges, some of which hardly may be overcome. These challenges are related to the impossibility of direct measurements of required parameters across large massifs. Even making boreholes provides limited information about the narrow vicinity of the borehole; for instance, measurements of the electrical conductivity and the porosity of the porous medium are generally not enough to reconstruct its permeability, which practically can not be measured directly. Thus, the problem actually turns into one of the recovery of relations between different (transport) parameters of the porous media. Generally, this problem is non-resolvable, because it requires thorough knowledge of the composition of the massif, its geological and seismic history, *etc.* Meanwhile, many recent studies deal with systems where the massif possesses a homogenous geological origin on the field scale [4–9]. Opportunities for an advance in the problem of reconstruction of relations between parameters for such kinds of systems might lay in the field of mathematical physics. In this study we wish to approach this problem in application to some important

geological systems, like ocean bed with methane hydrate deposits.

The ocean bed in regions with intense mud rain is very attractive and important for research due to bio- and geological richness and activity [4,5]; for example, these ocean bed systems host marine methane hydrate deposits. In such an ocean bed, sediments are exposed to a pressure load and have experienced a certain history of this load. These two factors result in compaction of the porous sediments. A typical sample of such a compaction, increasing with depth, can be seen in Fig. 1a, where the sediment porosity (ϕ) for different depths below the water-sediment interface is reported [4,5]. According to [6,7] one can fit the observed porosity with the exponential function

$$\phi(z) = \phi_0 \exp(-z/L), \quad (1)$$

where z is the depth below the water-sediment interface, L is the characteristic depth of compaction (see Caption to Fig. 1).

Earlier approaches to the relation between porosity and transport properties (such as, e.g., the Kozeny–Carman relation for flow [3,10]) adopted additional (though reasonable) constraints on the geometry of pore channels and utilized several characteristic parameters (for review see [3]). As well as the family of empirical equations relating permeability to porosity and irreversible water sat-

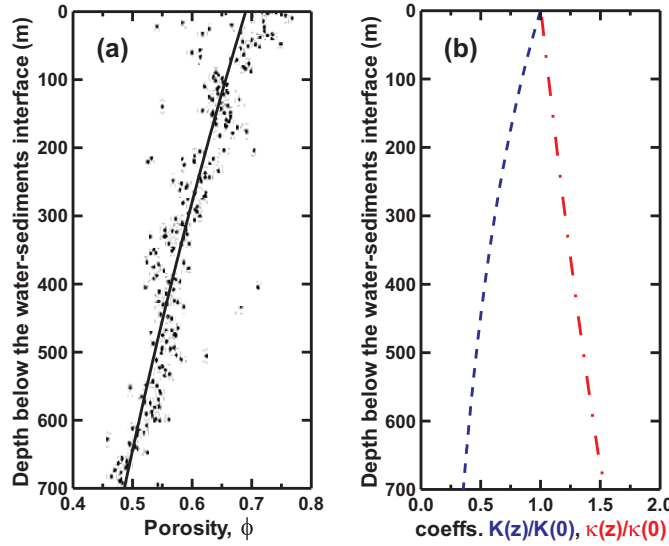


Fig. 1: (a) Observed porosity vs the depth below the water-sediment interface for the ODP (Ocean Drilling Program [4,5]) site 997 on the Blake Ridge crest—one of the largest marine hydrate provinces. The solid line represents the exponential decrease of the porosity (Eq. (1) with $\phi_0 = 0.69$ and $L = 2\text{ km}$ [6]). (b) Predicted permeability [blue dashed line, Eq. (4)] and thermal conductivity [red dash-dot line, Eq. (10)] of sediments.

uration [11], these models do not provide information on how the characteristic parameters will be transformed under compaction. Thus, a particular theory of the latter is remaining required.

In this Letter, in order to reconstruct the relations between parameters, we first argue for geometric features of compaction and corresponding scaling laws. Then we derive the dependence of transport coefficients on the porosity and, for a particular example, apply the derived dependence to examine whether the assumption of a linear temperature profile in sediments is adequate. We find that the amended predicted rate of the production of methane hydrate differs significantly from the “traditional” predictions assuming the linear temperature profile; this finding is of importance for the assessment of the planetary inventory of methane hydrate.

Physical model and scaling laws: Compaction of porous medium. — Prior to constructing a mathematical description of the problem, we need to establish physical features of the sediment compaction in Fig. 1a.

In general, when considering the variation of transport coefficients with porosity, one should keep in mind two critical thresholds for porosity [3]. First, there is a critical porosity important for acoustic processes in porous materials; a more porous material can be treated as a “suspension” and a less porous one is “solid”. This first critical porosity is material-specific and is typically near 0.5, *i.e.*, might be close to the lower edge of the part of the sediment column in Fig. 1. For porosities lower than the second threshold, chemical compaction is taking over the

mechanical one. This second transition occurs for porosities which are beyond the scope of our study. According to seismic data, for the part of the sediment column we consider, the first critical transition does not occur as well. Indeed, geological and mechanical structure of sediments is reported to be continuous enough for using the seismic wave reflection to detect as small volumetric fraction of bubbles in pores as 1–2% [5, 12, 13]. Hence, qualitative transitions in the structure of porous sediments are not expected.

The stress load on the system is anisotropic; the vertical direction is discriminated due to gravity. In a solid body the stress would be strictly anisotropic. However, the stress in granular materials (including cemented ones) is known to be not distributed homogeneously but to form force chains [14]. The stress along chains is much bigger than the average stress, and the grain displacements and deformations in the course of compaction are mainly driven by these chains. Meanwhile, the randomness of the geometry of contacts and the branching of force chains decreases the anisotropy of the network of force chains in comparison to the stress anisotropy for a solid body [14–16]. For simplicity, we assume the compaction process to be isotropic. Henceforth, we treat an isotropic compaction and consider the sediments to have similar geologic origin (which is reasonable for the geological systems we consider, on the timescale of several million years [5]).

In our model, as a first approach to the problem, we do not consider the fragmentation of sediment grains. Anisotropy of compaction and fragmentation are the main reasons for the change of the topology of the pore channels’ network. Without them, compaction affects this topology non-efficiently, but rather shrinks the channels. Further, the variation of the density of the solid matrix material is negligible against the background of the pore shrinking.

Let us derive general scaling laws for the compaction of sediments the physical features of which are described above. We consider a certain volume V of the porous medium and fix this volume to particles of the solid matrix (V changes due to compaction); L , l , and V_s stand for the total channels’ length in V , the characteristic channels’ diameter, and the volume of the solid material in V , respectively. Hence,

(i) porosity

$$\phi = \frac{L l^2}{V} = \frac{L l^2}{V_s + L l^2}, \quad \text{and thus} \quad L l^2 = \frac{\phi V_s}{1 - \phi}.$$

(ii) Owing to the unchanging shape of the channels’ network, $L^3 \propto V$.

(iii) Owing to the unchanging density of the solid material, $V_s = (1 - \phi)V$ is constant in the course of compaction; therefore $V \propto (1 - \phi)^{-1}$ and

$$L \propto \frac{1}{(1 - \phi)^{1/3}}. \quad (2)$$

From (i),

$$l^2 \propto \frac{\phi}{1-\phi} \frac{1}{L} \propto \frac{\phi}{(1-\phi)^{2/3}}. \quad (3)$$

These relations are obviously relevant for a tube model of the porous medium. However, they are derived without actual relaying on features of any specific model and we expect them to be reasonably accurate for realistic geometric models of porous medium [17] as long as we deal with a sparse porous structure (in Fig. 1 porosity varies in the range from 0.5–0.7). The scaling of the linear measure l for realistic models describes the variation of transversal linear measures of pores. For low-porosity materials the actual scaling laws become sensitive to features of the pore geometry (e.g., see [17]).

Permeability. We use the definition of the permeability K according to the Darcy's law (e.g., see [2, 18]):

$$\vec{v}_f = -(K/\eta)\nabla p,$$

where \vec{v}_f is the *filtration velocity* of the fluid, η is the dynamic viscosity, p is pressure. When the distribution of the orientation of pore channels and topology of the pore network are unchanged—as they are in our model of compaction—the fluid speed in pores $u_f \equiv \phi^{-1}v_f$ requires the pressure gradient proportional to l^{-2} . Thus, $v_f \propto \phi l^2 |\nabla p|$ and

$$K \propto \frac{\phi^2}{(1-\phi)^{2/3}}. \quad (4)$$

For instance, the data reported in Fig. 1 yield $K(\phi = 0.69)/K(\phi = 0.49) \approx 2.8$ due to compaction; that is the permeability of the upper sediment zone ($\phi \approx 0.69$) is by factor 2.8 larger than that at the bottom of the shown sediment column ($\phi \approx 0.49$).

Remarkably, in [9] a rough dependence of the permeability on the porosity, $K \propto \phi^2$ [cf Eq. (4)], was adopted because of the lack of reasonable theories on scaling laws for sediments experiencing compaction.

Molecular diffusion of solute. The evolution of the solution concentration C in quiescent pore water is governed by the equation

$$\frac{\partial}{\partial t}(\phi C) = \nabla \cdot [\gamma_D(\phi) D_m \nabla C], \quad (5)$$

where D_m is the molecular diffusivity of the solute in bulk, and $\gamma_D(\phi)$ is the geometric factor featuring the pore network.

Similarly to the permeability, the geometric factor for the molecular diffusivity (γ_D) depends on porosity ϕ which varies significantly with depth. The length of the channels L does not effect the diffusional flux until the statistics of channel orientations are changed. With the concentration gradient given, the solute flux through the area S is linearly proportional to the area of channel cross-section, S_{pore} :

$$\gamma_D \propto S_{\text{pore}}/S = \phi. \quad (6)$$

Recall, porosity ϕ is exactly the average value of S_{pore}/S . This becomes evident if one considers the cubic volume thinly sliced parallel to one of its sides; for each slice the fraction of the pore volume is S_{pore}/S , and, thus, for the whole cube volume the ratio of pore volume to the cube volume, which is porosity ϕ , is the average value of S_{pore}/S .

Hydrodynamic dispersion. Due to the irregularity of the microstructure of the pore network, the macroscopically uniform displacement of liquid results in a mixing flow in pores, which acts as an additional diffusion and is referred to as hydrodynamic dispersion [1, 19]. The hydrodynamic dispersion in an isotropic medium is strictly anisotropic; the longitudinal and lateral dispersion coefficients differ and are linearly proportional to the filtration speed v_f [19]:

$$D_{\parallel} = v_f d_{\parallel}, \quad D_{\perp} = v_f d_{\perp}.$$

For a steady viscous flow in pores, $D_{\parallel, \perp} \propto u_f^2 \tau_{\text{corr}} \propto u_f l_{\text{corr}}$ (recall, the fluid speed in pores $u_f = v_f/\phi$). For an isotropic compaction, l_{corr} is scaled as the pore network skeleton, that is $\propto L$, and Eq. (3) yields $D_{\parallel, \perp} \propto (v_f/\phi)L \propto v_f/[\phi(1-\phi)^{1/3}]$. Hence,

$$d_{1,2} \propto \frac{1}{\phi(1-\phi)^{1/3}}. \quad (7)$$

Notice, the geometric factor γ_D for molecular diffusion [Eq. (6)] and the hydrodynamic dispersion coefficients [Eq. (7)] are affected by the compaction differently.

Electrical conductivity. For the electrical conductivity one should clearly distinguish two cases: (i) sea water and (ii) pure water in pores. Due to electrolytes dissolved, sea water possesses the electrical conductivity about 5S/m which is much more than that of the porous-skeleton material. The current flows through the liquid volume. On the pore scale, this case is geometrically equivalent to the case of molecular diffusion. Indeed, for a steady diffusive flux we have the equation $\Delta C = 0$ for concentration C in the pore volume, zero normal derivative of C on the pore walls, and fixed mean (macroscopic) gradient of C ; for electrostatic potential φ we find the same equation $\Delta \varphi = 0$ in the pore volume with zero normal derivative of φ on the pore walls and fixed macroscopic gradient of φ . For the electrical conductivity σ of *sea water*, this equivalence yields

$$\sigma \propto \phi, \quad (8)$$

the same scaling law as Eq. (6). This law can be observed for $\phi \gtrsim 0.15$ in realistic models of the pore morphology and experiments (see Ref. [17] and references therein for experimental data).

The case of pure water is significantly more subtle. Without electrolytes dissociated, water has small number of charge carriers; the mineral surface conductivity can make significant contribution into the microscopic

electrical conductivity. For sands, experiments demonstrate nearly the same conductivity for wet massif and the massif fully saturated with pure water, which indicates that the electrical current flows along the water-mineral interface [20]. In this case, resistivity is mainly contributed by the sharp sand grain contacts; the geometry of these contacts is controlled by many factors, including the stress [21]. This problem is very complex and lies beyond the immediate applicability field of our results. Thus, we emphasize that Eq. (8) is valid for salt water only.

Heat diffusion. Heat transfer in the porous medium is governed by the equation

$$\frac{\partial}{\partial t}[(1 - \phi)\rho_s c_{P,s} + \phi\rho_f c_{P,f}]T + \nabla \cdot [\vec{v}_f \rho_f c_{P,f} T] = \nabla \cdot [\kappa(\phi) \nabla T], \quad (9)$$

where ρ_s , ρ_f and $c_{P,s}$, $c_{P,f}$ are the densities and the specific heat capacities of the solid matrix and the fluid, respectively, $\kappa(\phi)$ is the heat conductivity of the fluid-saturated medium.

An evaluation of the dependence of the macroscopic thermal conductivity on the porosity of sediments experiencing compaction is much more complicated than for the permeability and the solution diffusivity, because heat flows through both the solid matrix and the fluid in pores and the fluxes in these two subsystems (with complex random geometry) should be found and conjuncted at the interface. This issue requires a particularly accurate study. Straightforward scaling rules cannot be derived with our approach here and, instead, we relay on empirical relation suggested in Ref. [22] for porous media saturated with a weakly heat conducting fluid (such as air or water, which has 5–10 times smaller heat conductivity than typical mineral materials).

Chaudhary and Bhandari [22] reported the law

$$\kappa(\phi) = \kappa_s \left(\frac{\kappa_f}{\kappa_s} \right)^{1-n} \frac{[\phi(1 - \phi)]^n}{\phi + (1 - \phi)\kappa_f/\kappa_s}, \quad (10)$$

where κ_f and κ_s are the conductivities of matrix material and fluid in pores, respectively, and $n = 0.5(1 - \ln \phi)/\ln[\phi(1 - \phi)\kappa_s/\kappa_f]$, to be satisfactory accurate for a broad variety of sediment-kind porous materials. For our study of carbon-bearing sediments, the relevant matrix material heat conductivity is $\kappa_s = 2.93 \text{ J/(ms K)}$ [22] (for water $\kappa_f = 0.58 \text{ J/(ms K)}$ is well known). In particular, for the porosity profile in Fig. 1, $\kappa(\phi = 0.69)/\kappa(\phi = 0.49) \approx 0.66$, *i.e.*, the temperature profile slope varies by factor 1.5 for different parts of the sediment column.

Geothermal gradient and methane hydrate inventory. – While the researchers modelling methane hydrate deposits (*e.g.*, [6–9]) adopt a uniform geothermal gradient $G := dT/dz$, it is, in fact, nonuniform. Instead, the heat flux, which is the product of the geothermal gradient and the (nonuniform) thermal conductivity, is uniform

under time-independent conditions. Hence,

$$G(z) \equiv \frac{dT(z)}{dz} = \frac{[\text{heat flux}]}{\kappa(z)} = \frac{\kappa(0)}{\kappa(z)} \frac{dT(0)}{dz}. \quad (11)$$

Eq. (11) yields

$$T(z) = T(0) + G_0 \int_0^z \frac{\kappa(0)}{\kappa(z_1)} dz_1, \quad (12)$$

where G_0 is the geothermal gradient next to the water-sediment interface. The latter expression is convenient when G_0 is directly measured in shallow upper layer of sediments. However, for sediments bearing methane hydrate, the geothermal gradient is practically derived in a different way.

Immediately below the floor of deep seas the pressure of the water column is large enough and the temperature is low enough for methane hydrate to be stable. Deeper into sediments the temperature grows and, at certain depth, the pressure becomes not sufficiently large to stabilize the hydrate (the critical pressure depends on temperature nearly exponentially [23]). Thus, the Hydrate Stability Zone (HSZ) spreads in sediments from the water-sediment interface down to a certain depth, the base of the HSZ, which is detected by the reflection of seismic waves [12]. Practically, for marine methane hydrates the geothermal gradient is inferred from the position $z = L_h$ of the base of the HSZ [6, 7]: $G := (T(L_h) - T(0))/L_h$, where $T(L_h)$ is calculated as the hydrate destabilization temperature for the known water salinity and hydrostatic pressure $P(L_h)$ of the water column (*e.g.*, one can employ an accurate mathematical model of hydrate from [24]). For this case,

$$T(z) = T(0) + (T(L_h) - T(0)) \frac{\int_0^z \kappa^{-1}(z_1) dz_1}{\int_0^{L_h} \kappa^{-1}(z_1) dz_1}. \quad (13)$$

In Fig. 2a, the temperature profile consistent with compaction is compared to “traditional” linear profiles guessed either from the observed position of the base of HSZ or from measurements of the sediments temperature profile next to the water-sediment interface. Remarkably, assuming the geothermal gradient being uniform is especially inaccurate for the latter case (red dotted line): the assumption of the linear profile significantly rises the base of the HSZ.

The role of the nonuniformity of G appears to be especially pronounced in the problem of hydrate formation. When a hydrate is present in the HSZ, (i) the concentration of methane dissolved in water is determined by the thermodynamic equilibrium between the hydrate and the aqueous solution, in other words, it equals the solubility, and (ii) the diffusive flux of the aqueous methane may possess non-zero divergence equal to the formation/dissociation rate of hydrate in pore water (up to a known constant multiplier determining the fraction of methane in hydrate). We employed the thermodynamic model of a hydrate developed in [24] for the calculation of

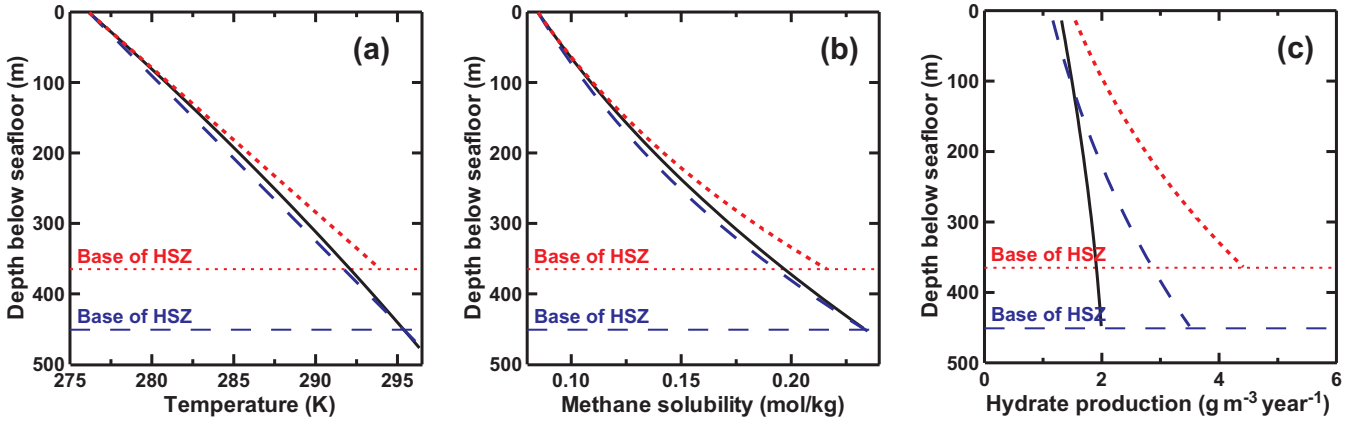


Fig. 2: (Color on-line) Predictions for the data in Fig. 1: Temperature profiles (a), the aqueous methane solubility in equilibrium with hydrate (b), and the consequent production of methane hydrate due to diffusion of methane dissolved in pore water (c) for an accurate nonuniform geothermal gradient (black solid lines), and for simplified linear temperature profiles guessed either from the observed position of the base of HSZ (blue dashed lines) or from the observed geothermal gradient immediately next to the water-sediment interface (red dotted lines).

the solubility profiles (Fig. 2b) and then derived the contribution of this flux into the hydrate production (Fig. 2c). In addition, to calculate the divergence of the diffusive flux we accounted for the strong dependence of the methane molecular diffusivity on the temperature (the dependence on pressure is negligible): $D_m \approx (7 + 0.4K^{-1}(T - 273.15K) + 10^{-3}K^{-2}(T - 273.15K)^2) \cdot 10^{-10}m^2/s$, which fits well with experimental data (*e.g.*, [25]). One can see, that linear temperature profiles significantly overestimate the production of methane hydrate in the lower part of the HSZ. Thus, the results of mathematical modelling which simultaneously considers the compaction of the sediment and ignores the consequent non-linearity of the temperature profile (*e.g.*, [6–9]) are significantly affected by this inconsistency.

Notice, here we argue for the importance of the scaling laws for compaction and assess the physical accuracy of models adopted in [6–9] in this context only. This is the reason, why we readdress the pure Fickian diffusion of aqueous methane and do not consider non-Fickian effects, thermodiffusion and gravitational stratification of the solute, ignored in the existing models of the formation of hydrate deposits, although the importance of non-Fickian effects was shown in [26, 27].

Conclusion. – Summarizing, we have described an isotropic compaction of porous medium and derived scaling laws for geometrical properties of the pore structure. These laws have yielded dependencies of transport properties [permeability, Eq. (4), effective molecular diffusivity, Eq. (6), hydrodynamic dispersion, Eq. (7), electrical conductivity, Eq. (8), and thermal conductivity, Eq. (10)] on the porosity for porous sediments of similar geological origin. Notably, the compaction of sediments (for example, see Fig. 1a) is an inherent feature of most geological systems on the field scale. In particular, for paradigmatic models of formation of marine methane hydrate [6–9],

compaction is a “key ingredient”. The employment of our results for transport coefficients provides an opportunity for a significant enhancement of physical soundness and relevance of the modelling of sediments experiencing compaction and, in particular, the global methane hydrate inventory (*e.g.*, Fig. 2c demonstrates the inaccuracy of the hydrate production rate in treatments disregarding the variation of the thermal conductivity due to compaction).

I thank N. V. Brilliantov, L. S. Klimenko, D. Packwood, J. Levesley, J. Rees, and P. Jackson for fruitful discussions and comments. The work has been supported by NERC Grant no. NE/F021941/1.

REFERENCES

- [1] SAHIMI M., *Rev. Mod. Phys.*, **65** (1993) 1393.
- [2] NIELD D. A. and BEJAN A., *Convection in Porous Media* 3rd Edition (Springer) 2006.
- [3] MAVKO G., MUKERJI T. and DVORKIN J., *The Rock Physics Handbook* 2nd Edition (Cambridge University Press) 2009.
- [4] PAULL C. K., MATSUMOTO R., WALLACE P. J. and *et.al.*, *Proceedings of the Ocean Drilling Program, Initial Results*, Vol. **164** (College Station, TX (Ocean Drilling Program)) 1996.
- [5] PAULL C. K., MATSUMOTO R., WALLACE P. J. and DILLON W. P. (Editors), *Proceedings of the Ocean Drilling Program, Scientific Results*, Vol. **164** (College Station, TX (Ocean Drilling Program)) 2000.
- [6] DAVIE M. K. and BUFFETT B. A., *J. Geophys. Res.*, **106** (2001) 497.
- [7] DAVIE M. K. and BUFFETT B. A., *J. Geophys. Res.*, **108** (2003) 2495.
- [8] ARCHER D., *Biogeosciences*, **4** (2007) 521.

- [9] GARG S. K., PRITCHETT J. W., KATOH A., BABA K. and FUJII T., *J. Geophys. Res.*, **113** (2008) B01201.
- [10] CARMAN P. C., *L'écoulement des Gaz á Travers les Milieux Poreux. Bibliothèque des Sciences et Techniques Nucléaires* (Presses Universitaires de France, Paris) 1961.
- [11] SCHLUMBERGER LIMITED, *Log Interpretation Principles/Applications* (Schlumberger Wireline & Testing, Houston, TX) 1991.
- [12] MACKAY M. E., JARRARD R. D., WESTBROOK G. K. and HYNDMAN R. D., *Geology*, **22** (1994) 459.
- [13] HOVLAND M., FRANCIS T. J. G., CLAYPOOL G. E. and BALL M. M., *JOIDES Journal*, **25** (1999) 20.
- [14] LIU C. H., NAGEL S. R., SCHECTER D. A., COPPERSMITH S. N., MAJUMDAR S., NARAYAN O. and WITTEN T. A., *Science*, **269** (1995) 513.
- [15] BOUCHAUD J., CLAUDIN P., LEVINE D. and OTTO M., *Eur. Phys. J. E*, **4** (2001) 451.
- [16] GENG J., REYDELLET G., CLÉMENT E. and BEHRINGER R. P., *Physica D*, **182** (2003) 274.
- [17] ROBERTS J. N. and SCHWARTZ L. M., *Phys. Rev. B*, **31** (1985) 5990.
- [18] WHITAKER S., *Water Resour. Res.*, **1** (1986) 3.
- [19] SAFFMAN P. G., *J. Fluid. Mech.*, **6** (1959) 321.
- [20] REVIL A. and GLOVER P. W. J., *Geophys. Res. Lett.*, **25** (1998) 691.
- [21] HERTZ H., *J. f. reine u. angewandte Math.*, **92** (1882) 156.
- [22] CHAUDHARY D. R. and BHANDARI R. C., *J. Phys. D: Appl. Phys.*, **2** (1969) 609.
- [23] MORIDIS G., *Soc. Petrol. Eng. J.*, **32** (2003) 359.
- [24] SUN R. and DUAN Z., *Chem. Geol.*, **244** (2007) 248262.
- [25] SACHS W., *J. Pet. Sci. Eng.*, **21** (1998) 153.
- [26] GOLDOBIN D. S. and BRILLIANTOV N. V., *unpublished, E-print arXiv:1011.5140*, (2011) .
<http://arxiv.org/abs/1011.5140>
- [27] GOLDOBIN D. S., BRILLIANTOV N. V., LEVESLEY J., LOVELL M. A., ROCHELLE C. A., JACKSON P., HAYWOOD A., HUNTER S. and REES J., *unpublished, E-print arXiv:1011.6345*, (2011) .
<http://arxiv.org/abs/1011.6345>